

Efficient Scalar Quantization for MIMO Spatial Multiplexing Receivers

Francisco A. Monteiro^{1,2}, Ian J. Wassell²

¹*Department of Engineering, University of Cambridge*

²*Digital Technology Group, The Computer Laboratory, University of Cambridge
15 JJ Thomson Avenue, Cambridge CB3 0FD, United Kingdom*

{fatbnm2, i jw24}@cam.ac.uk

Abstract— The maximum likelihood detection of multiple input multiple output (MIMO) spatial multiplexing systems is strongly limited by its complexity. We propose that a quantized version of this problem permits the multiplications involved in the numerous calculations of Euclidean distances to be replaced by the use of a small look-up table storing all the exact possible distance components in each dimension of the quantized receive space. The number of pre-stored elements is as small as the number of quantization levels per dimension. This paper presents an approximate analysis of the quantization error which allows us to understand the results from simulations performed over fast flat fading channels for different MIMO systems.

I. INTRODUCTION

MIMO systems [1], [2], make use of the existence of different channels between the transmitter and the receiver due to the existence of multipath propagation in the channel. The systems can be designed in order to exploit that diversity either to maximize the diversity of the link (space-time coding systems) or to maximize the overall bit throughput (spatial multiplexing systems). Tradeoffs between the two frameworks have been under investigation and a scheme commuting between the two has been recently proposed [3]. Spatial multiplexing allows the bit rate of wireless links to be greatly increased; however this comes at the expense of an enormous rise in the complexity of optimum detection as the number transmitting antennas is increased and modulations with higher spectral efficiency are used. For the case of equally probable symbols the maximum a posteriori (MAP) detection strategy corresponds to the maximum likelihood (ML) criterion, leading to a number of comparisons that grows exponentially with the number of transmission antennas. For this reason, sub-optimal receivers have always been fundamental for spatial multiplexing, leading to both linear and non-linear receivers [2], [4], encompassing a range of different power performance profiles. Receivers using the zero-forcing (ZF) or the minimum mean square error (MMSE) criteria constitute the linear receivers whilst the most used example of non-linear receivers is the vertical Bell Laboratories layered space-time receiver (BLAST), also called the ordered successive interference cancellation (OSIC) receiver [4], [5]. Nevertheless, their sub-optimality leads to a loss in the diversity extracted by the system, i.e., the curves representing the number of errors against the signal to noise ratio (SNR) are less steep. The call for near ML performance originated research into other low complexity methods where sphere decoding [4], and lattice reduction [5], [6] are the most

prominent examples. The latter retains the diversity of ML, exhibiting performance curves parallel to those of ML (corresponding to a power penalty) at only a fraction of the computational cost. Attempts to simplify the brute force approach used by ML receivers are always limited by the number comparisons needed, and assessments of the complexity of the algorithms are chiefly made by counting the total number of multiplications required in the detection [7].

This paper presents a technique to simplify the calculation of the squared Euclidean distances required in ML detection. The technique requires the scalar quantization of both the received lattice (in each different channel realisation) and the received vector. This scalar quantization is performed in each dimension (i.e., component) of both the lattice points and the received vector. The presented approach contrasts with the ones involving vector quantization in MIMO [8 and references therein], which is inherently much more complex than performing scalar quantization in each dimension which can be implemented in parallel. Vector quantization is impaired by the slow convergence of the iterative Linde-Buzo-Gray (LBG) algorithm [9-Chapter 5] that is needed to run for every different channel realization in order to find the best set of vector codewords. The proposal in this paper is inspired by similar problems in computer graphics and image processing where approximations for the Euclidean distance are used [10], [11] (not for the squared Euclidean distances though). Note that this type of computational problem which involves the repeated use of non trivial operations gave rise to the approximation that modifies the forward-backward MAP algorithm into the max-log MAP algorithm [12-Sec.4.3]. The application of completely multiplication-free Euclidean distances have been used in MIMO with minimum penalty [13], however in that case the approximation occurs for the l_2 norm in the bidimensional space of the transmitted constellation. Instead, this paper proposes the simplification of the evaluation of the Euclidean distances in the received hyper dimensional space where the ML search is undertaken. The key component is a look-up table technique originally proposed to speed up the calculation of squared Euclidean distances in vector quantization [14], [15].

II. TRADITIONAL RECEIVERS

A MIMO system under flat fading can be represented in a complex baseband model as

$$\mathbf{y} = \mathbf{H}\mathbf{x} + \mathbf{n}_g, \quad (1)$$

where $\mathbf{x} = [\mathbf{x}_1, \mathbf{x}_2, \dots, \mathbf{x}_{N_T}]^T$, that is, each component is transmitted from each one of the N_T transmitter antennas, $\mathbf{y} = [\mathbf{y}_1, \mathbf{y}_2, \dots, \mathbf{y}_{N_R}]^T$, where each component corresponds to the signal in each one of the N_R receiver antennas and the noise vector $\mathbf{n}_g = [\mathbf{n}_{g,1}, \mathbf{n}_{g,2}, \dots, \mathbf{n}_{g,N_R}]^T$ is composed of complex Gaussian random variables with zero mean and variance $\sigma_{n_g}^2$ (i.e., $\sigma_{n_g}^2/2$ in both real and imaginary parts).

The channel matrix \mathbf{H} for this $n_R \times n_T$ system is

$$\mathbf{H} = \begin{bmatrix} h_{11} & h_{12} & \dots & h_{1N_T} \\ h_{21} & h_{22} & \dots & h_{2N_T} \\ \vdots & \vdots & \ddots & \vdots \\ h_{N_R1} & h_{N_R2} & \dots & h_{N_RN_T} \end{bmatrix} \quad (2)$$

where all the elements are i.i.d complex circularly symmetric Gaussian random variables with zero mean and unit variance (i.e., with variance 0.5 in both the real and imaginary components). The components in \mathbf{x} are taken from a set Ξ_C of symbols belonging to an M -ary complex constellation with real and imaginary parts taken from the real set Ξ_R . We impose an average signal power $\sigma_x^2 = 1$ for the symbols taken from the constellation Ξ_C . Thus, for a given SNR, the noise power $\sigma_{n_g}^2$ is determined by the relation

$$\text{SNR} = \frac{\mathbb{E}_{\mathbf{H}, \mathbf{x}} \left\{ \|\mathbf{H}\mathbf{x}\|^2 \right\}}{\mathbb{E}_{\mathbf{n}} \left\{ \|\mathbf{n}\|^2 \right\}} = \frac{N_T N_R \sigma_x^2}{N_R \sigma_{n_g}^2} = \frac{N_T}{\sigma_{n_g}^2}. \quad (3)$$

This model can be converted into one with the double number of dimensions where all the elements are real numbers by stacking the real and imaginary parts of \mathbf{x} and \mathbf{y} and constructing a new equivalent channel matrix

$$\begin{bmatrix} \Re \mathbf{y} \\ \Im \mathbf{y} \end{bmatrix} = \begin{bmatrix} \Re \mathbf{H} & -\Im \mathbf{H} \\ \Im \mathbf{H} & \Re \mathbf{H} \end{bmatrix} \begin{bmatrix} \Re \mathbf{x} \\ \Im \mathbf{x} \end{bmatrix} + \begin{bmatrix} \Re \mathbf{n} \\ \Im \mathbf{n} \end{bmatrix} \quad (4)$$

where the symbols \Re and \Im indicate the real and imaginary components respectively. Equation (1) can be written as

$$\mathbf{y}_r = \mathbf{H}_r \mathbf{x}_r + \mathbf{n}_r. \quad (5)$$

Thus $\mathbf{x}_r = [\mathbf{x}_{r,1}, \mathbf{x}_{r,2}, \dots, \mathbf{x}_{r,2N_T}]^T$, $\mathbf{y}_r = [\mathbf{y}_{r,1}, \mathbf{y}_{r,2}, \dots, \mathbf{y}_{r,2N_R}]^T$, and $\mathbf{n}_r = [\mathbf{n}_{r,1}, \mathbf{n}_{r,2}, \dots, \mathbf{n}_{r,2N_R}]^T$. Also, \mathbf{H}_r doubles the dimensions with respect to \mathbf{H} . The problem of detecting the transmitted symbols is optimally solved by the maximum likelihood procedure based in squared Euclidean distances, i.e.,

$$\hat{\mathbf{x}}_{r(ML)} = \min_{\mathbf{x}_r \in \Xi_{2N_T}^{\mathbb{R}}} \left\{ \|\mathbf{y}_r - \mathbf{H}_r \mathbf{x}_r\|^2 \right\}. \quad (6)$$

This implies the measurement and comparison of M^{N_T} squared Euclidean distances per component of the \mathbf{R}^{2N_R} space or per component of the complex space \mathbf{C}^{N_R} in (1).

Hence, the search increases exponentially with the number of transmission antennas for a given modulation.

The simplest linear receiver corresponds to a ZF criterion, i.e., an inversion of the channel matrix. In the general case, as the channel matrix \mathbf{H} is not necessarily square (corresponding to $N_T = N_R$), then the Moore-Penrose pseudo-inverse of \mathbf{H} is used, which is given by $\mathbf{H}^+ = (\mathbf{H}^H \mathbf{H})^{-1} \mathbf{H}^H$ where $(\cdot)^H$ denotes the Hermitian transposition. In this case the ‘‘filtering’’ matrix is

$$\mathbf{W}_{ZF} = \mathbf{H}^+. \quad (7)$$

This procedure induces noise enhancement in the constellation space where the decisions of constellation symbols are to be made. The MMSE receiver takes the noise into account, resulting in the following ‘‘filtering’’ matrix

$$\mathbf{W}_{MMSE} = \left(\mathbf{H}^H \mathbf{H} + \frac{1}{\text{SNR}} \mathbf{I}_{n_T} \right)^{-1} \mathbf{H}^H. \quad (8)$$

The OSIC-ZF receiver uses (7) in an initial iteration. The component of \mathbf{y}_r with the smallest noise amplification by the corresponding row of \mathbf{W}_{ZF} is selected and detected. The next step is to remodulate that symbol and subtract its effect from the original received \mathbf{y}_r . This procedure is repeated for the new signal, originating the detection of a second component of \mathbf{y}_r , and is repeated until all components have been detected. The OSIC-MMSE receiver operates similarly by applying (8) instead of (7). The complexity of OSIC is only polynomial with N_T [7] but the fact that an erroneous decision in one component cascades the error throughout the components to be subsequently detected explains the fact that OSIC is not able to entirely exploit the diversity available in the system.

III. MULTIDIMENSIONAL SCALAR QUANTIZATION

The proposed receiver starts by stacking the imaginary components of \mathbf{y} , generating \mathbf{y}_r , as considered in (5). Then the received N_R -dimensional space is quantized and all the possible points on the lattice are mapped into the quantized space. The possible points in the lattice are $\mathbf{y}_r^{(l)} = \mathbf{H}_r \mathbf{x}_r^{(l)}$ $l=1, 2, \dots, M^{N_T}$. Denoting the quantization process by $\mathcal{Q}(\cdot)$, the resulting quantized received vector is

$$\tilde{\mathbf{y}}_r = [\tilde{y}_{r,1}, \tilde{y}_{r,2}, \dots, \tilde{y}_{r,2N_R}]^T = \mathcal{Q}([\mathbf{y}_{r,1}, \mathbf{y}_{r,2}, \dots, \mathbf{y}_{r,2N_R}]^T). \quad (9)$$

Each one of these components $\tilde{y}_{r,i} \in \{c_1, c_2, c_3, \dots, c_L\}$, which are the $L=2^b$ possible quantization levels (described by b bits) with a uniform step

$$q = c_m - c_{m+1}, \quad m \in \{1, 2, \dots, L\}. \quad (10)$$

The Euclidean distances needed in (5) are approximated by

$$\|\tilde{\mathbf{y}}_r - \tilde{\mathbf{y}}_r^{(l)}\|^2 = \sum_{i=1}^{N_R} (\tilde{y}_{r,i} - \tilde{y}_{r,i}^{(l)})^2 = \sum_{i=1}^{N_R} \Delta_i^2, \quad l=1, 2, \dots, M^{N_T}. \quad (11)$$

For a particular lattice point $\tilde{\mathbf{y}}_r^{(l)}$, and defining $\Delta_i = (\tilde{y}_{r,i} - \tilde{y}_{r,i}^{(l)})$, each particular squared Euclidean distance is

$$d^2 = \sum_{i=1}^{N_R} \Delta_i^2. \quad (12)$$

In [14] the authors consider a unitary increment q and positive c_i whereas we propose that q can be any integer. The simulations were implemented considering the levels $\{c_1, c_2, c_3, \dots, c_L\} = \{-(L-1), \dots, -3, -1, +1, +3, \dots, (L-1)\}$. In fact, the restriction to $q=1$ would bring difficulties to the implementation of the technique that will be presented in the next section. Each component of $\mathbf{y}_r^{(l)}$ can be either positive or negative and therefore $Q(\cdot)$ should be able to deal with both cases. The extension to negative components would require a central zero level and hence an even number of levels.

Fig. 1 (a) depicts the appropriate bipolar quantizer. It should be noticed that both the received signal and the lattice itself can be bounded to $[-y_{i,sat}, +y_{i,sat}]$ in the i^{th} real dimension, corresponding to the clipping imposed by $Q(\cdot)$. This maximum value could be $y_{i,sat} = \max\{y_{r,i}^{(l)}\}$ in each component and updated in each channel realization, however we will make them all equal to $y_{sat} = \max\{y_{r,i}^{(l)}\}$ taken over all the real lattice points. This creates an hypercube with edges having size $2y_{sat}$.

The look-up technique to be presented in Section V was originally proposed in [14] for vector quantization considering the quantizer of Fig. 1 (b). However it is inappropriate for the MIMO situation as it would require shifting each one of the complex lattices (comprising M^{N_r} points in each received dimension) by $\frac{y_{sat}}{2} + i \frac{y_{sat}}{2}$.

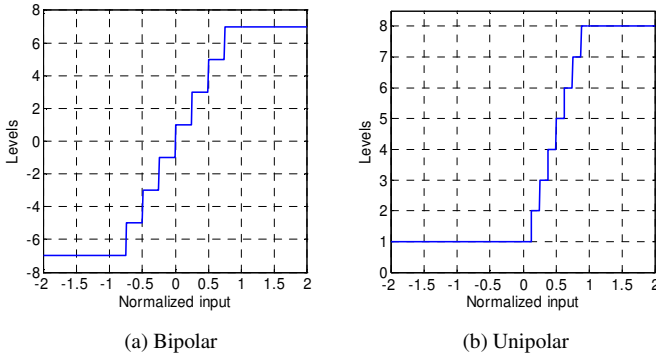


Fig. 1. Quantizer with $L=8$ levels (3 bits) for each dimension normalizing the input to y_{sat} .

IV. MULTIDIMENSIONAL QUANTIZATION ERROR

In this section we quantify the effect of the quantization described in Section III. We will introduce some assumptions that will greatly simplify the analysis in order to allow us to extend the analysis of scalar quantizers (e.g. [9-Chapter 5]) to the case of MIMO detection.

A. Uncorrelated noise and uncorrelated dimensions

Given the stacked model (4)-(5), this assumption means that not only the signals in the different antennas are

uncorrelated but also that their real and imaginary components are also uncorrelated. Moreover, we assume that the quantization noise, n_q , is independent of both the received signal \mathbf{y}_r and the lattice points $\mathbf{y}_r^{(l)}$. These two assumptions allow the total variance (or power) of the *total noise* in a quantized vector to be written as

$$\sigma_{n_q}^2 = \sigma_{n_q,1}^2 + \sigma_{n_q,2}^2 + \dots + \sigma_{n_q,i}^2 + \dots + \sigma_{n_q,N_R}^2. \quad (13)$$

where $\sigma_{n_q,i}^2$ is the variance of the *quantization noise* in the i^{th} dimension.

B. Saturation does not impair detection

The complex lattice of possible points in each receive antenna is a combination of N_T constellation points drawn from Ξ_C weighted by the complex Gaussian probability density functions of the respective row in (2). If the hypercube defined by the side y_{sat} contains all the lattice points, then the *saturation noise* does not introduce any degradation in the ML problem. Consider the example in Fig. 2 which shows the complex lattices for each receive antenna of a 2×2 system using a traditional QPSK constellation and the channel matrix

$$\mathbf{H} = \begin{bmatrix} -0.3+0.5i & 0.3-0.2i \\ -0.6+2i & 1+2i \end{bmatrix}. \quad (14)$$

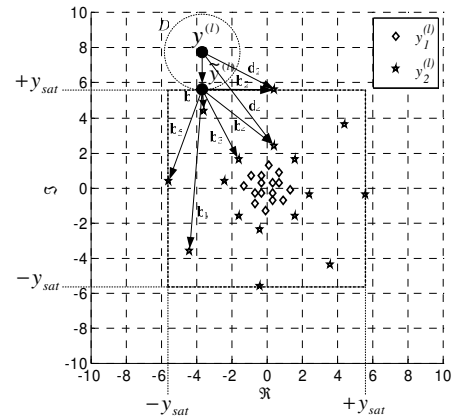


Fig. 2. The complex lattices in the two complex components of a 2×2 system with QPSK symbols ($M^{N_r} = 16$).

The effect of saturation will give rise to a quantized point in one of the faces of the hypercube. As can be seen in the 4 (real) dimensional case depicted in Fig. 2, the closest lattice point can only lie at the intersection of the bounded subspace and the hypersphere D which actually is the projection of \mathbf{y} in the closest side of the hypercube. So, the original k^{th} distance can be expressed in terms of the distance to the projection and the remaining k^{th} distance \mathbf{b}_k : $\mathbf{d}_k = (\tilde{\mathbf{y}} - \mathbf{y}) + \mathbf{b}_k$. Because $(\tilde{\mathbf{y}} - \mathbf{y})$ is fixed and it is impossible to have a lattice point inside D , then minimizing of \mathbf{d}_k or \mathbf{b}_k yields the same solution.

C. Uniform error per component

As a consequence of assumption B, the only cause of degradation in the performance will be caused by the granular

noise. Considering that the quantization in each dimension is described by a uniform error distribution, it is straightforward to obtain the well known expression for the quantization noise power (e.g. [9-Chapter 5])

$$\sigma_q^2 = \int_{-q/2}^{q/2} \frac{1}{q} x^2 dx = \frac{q^2}{12}. \quad (15)$$

Independently of the number of dimensions N_R , the mean error per dimension obtained by simulation using

$$E\{n_q\}_{[\%]} = E\left\{1 - \frac{\|\tilde{\mathbf{y}}_r - \tilde{\mathbf{y}}_r^{(l)}\|^2 - \|\mathbf{y}_r - \mathbf{y}_r^{(l)}\|^2}{\|\mathbf{y}_r - \mathbf{y}_r^{(l)}\|^2}\right\} \cdot 100 \quad (16)$$

is depicted in Fig. 3.

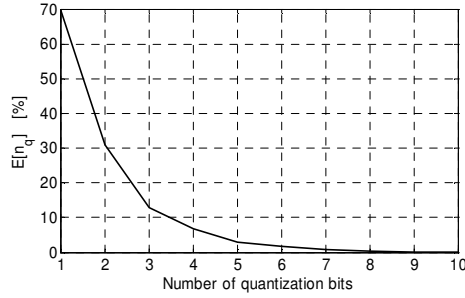


Fig. 3. Quantization error for the squared Euclidean distance as a function of the number of quantization levels specified by the number of bits required.

Using (13) and (15), the signal to total quantization noise ratio can be obtained by

$$\frac{\sigma_x^2}{\sigma_{N_i}^2} = \frac{\sigma_x^2}{\sigma_{N_q}^2} = \frac{\sigma_x^2}{\sum_{i=1}^{N_R} \frac{q_i^2}{12}} = \frac{\sigma_x^2}{\sum_{i=1}^{N_R} \frac{(2y_{i,sat}/L)^2}{12}} = \frac{3L^2\sigma_x^2}{\sum_{i=1}^{N_R} y_{i,sat}^2}. \quad (17)$$

D. Equal saturation in the dimensions (hypercube)

When $y_{i,sat}$ is made the same in all the N_R dimensions, (17) yields

$$\frac{\sigma_x^2}{\sigma_{n_q}^2} = \frac{3L^2\sigma_x^2}{N_R y_{sat}^2} = 3 \cdot \frac{(2^b)^2}{N_R} \cdot \left(\frac{\sigma_x}{y_{sat}}\right)^2. \quad (18)$$

or, equivalently,

$$\left(\frac{\sigma_x^2}{\sigma_{n_q}^2}\right)_{dB} = 4.77 + 6.02b - 10\log_{10}(N_R) + 20\log_{10}\left(\frac{\sigma_x}{y_{sat}}\right). \quad (19)$$

Expression (19) shows that when N_R doubles the quantization noise increases by 3 dB. On the other hand, every extra bit used in the quantization of each component improves the signal to quantization noise on that component by 6 dB. Thus, when increasing the N_R from 2 antennas to 4, only 0.5 extra bits would be necessary to compensate the loss and obtain the same performance of the 2×2 system (see Fig. 4).

A second outcome from (19) is that the last term implies that use of an equal y_{sat} which leads to a very poor performance in the antennas with compact lattices. Indeed, Fig. 2 corresponds to such a case: the total power in the first row of (14) leads to a much more compact lattice in first receive antenna, i.e., $E\{(y_{r,1}^{(l)})^2\} \ll E\{(y_{r,2}^{(l)})^2\}$.

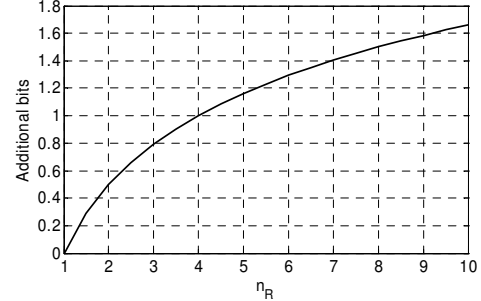


Fig. 4. Additional bits required to compensate the loss introduced by more receive antennas (i.e., dimensions), as defined by $6.02b = 10\log(N_R)$.

V. LOOK-UP TABLE TECHNIQUE

All the possible values of the distance components Δ_i^2 in (11) are an element of the matrix

$$\Omega^{(1)} = \begin{bmatrix} (c_1 - c_1)^2 & (c_1 - c_2)^2 & (c_1 - c_3)^2 & \cdots & (c_1 - c_L)^2 \\ (c_2 - c_1)^2 & (c_2 - c_2)^2 & (c_2 - c_3)^2 & \cdots & (c_2 - c_L)^2 \\ (c_3 - c_1)^2 & (c_3 - c_2)^2 & (c_3 - c_3)^2 & \cdots & (c_3 - c_L)^2 \\ (c_4 - c_1)^2 & (c_4 - c_2)^2 & (c_4 - c_3)^2 & \cdots & (c_4 - c_L)^2 \\ \vdots & \vdots & \vdots & \ddots & \vdots \\ (c_L - c_1)^2 & (c_L - c_2)^2 & (c_L - c_3)^2 & \cdots & (c_L - c_L)^2 \end{bmatrix}. \quad (20)$$

An inspection of $\Omega^{(1)}$ allows us to notice its expected symmetry and, furthermore, that it is possible to re-write it as

$$\Omega^{(2)} = \begin{bmatrix} 0 & (c_1)^2 & (c_2)^2 & \cdots & (c_{L-1})^2 \\ (c_1)^2 & 0 & (c_1)^2 & \cdots & (c_{L-2})^2 \\ (c_2)^2 & (c_1)^2 & 0 & \cdots & (c_{L-3})^2 \\ (c_3)^2 & (c_2)^2 & (c_1)^2 & \cdots & (c_{L-4})^2 \\ \vdots & \vdots & \vdots & \ddots & \vdots \\ (c_{L-1})^2 & (c_{L-2})^2 & (c_{L-3})^2 & \cdots & 0 \end{bmatrix}. \quad (21)$$

The elements of this matrix can be seen to be associated with the values of the quantization levels by $\Omega_{m,n}^{(2)} = (c_{|m-n|})^2$. Moreover, all the entries in $\Omega^{(2)}$ (i.e., all the squared distance components) belong to the ordered set

$$\Omega = [0, (c_1)^2, (c_2)^2, (c_3)^2, \dots, (c_{L-2})^2, (c_{L-1})^2]^T. \quad (22)$$

Using the rule

$$\Omega_{m,n}^{(1)} = \Omega_{m,n}^{(2)} = \Omega_a, \quad \text{with } a = \left(\frac{|c_m - c_n|}{q} + 1\right) \quad (23)$$

it is possible to locate and read the value of the distance component Δ_i^2 from the values pre-stored in Ω . Note that the division by q in (23) converts the true separation of the two components into the integer number of intervals between them.

It should be emphasised that the technique using this *non-truncated* look-up table does not introduce any errors in addition to the ones described in Section IV as it is an exact method in the quantized space. The authors in [14] and [15], proposed a *truncated* table to replace Ω , however this would not be useful in the context of MIMO detection.

VI. SIMULATION RESULTS

Simulation results for the receiver using maximum likelihood in the quantized space (MLQS) are presented in Figures 5, 6, 7 and 8 for different systems using QPSK and 16-QAM modulations and symmetric configurations (i.e., with $N_T = N_R$). All figures include the performance of the proposed receiver for different values of the number of bits per component and also the performances obtained using the traditional receivers (ZF, MMSE and OSIC with ZF or MMSE criterion) as well as the performance obtained using ML. The measure of the performance used in this paper is the symbol error rate (SER) instead of the bit error rate (which for QPSK is about half of the SER if Gray mapping is used as when one symbol is detected in error only one of the 2 bits will be incorrect). The simulations were checked against other results available in the literature: for QPSK the traditional receivers and ML can be compared with [2] for 2×2 and with [5], [7], for 4×4 ; for 16 QAM with 2×2 antennas the curves can be checked in [16].

The analysis in Section IV estimates the error involved in the quantization process. As always, the performance analysis also needs to include the effect of the Gaussian noise introduced in (1) and defined in (3). Since these noise sources are independent, the effective noise power is given by summing the respective noise powers. Consequently, the overall SNR is

$$\left(\frac{\sigma_x^2}{\sigma_{n_t}^2} \right)^{-1} = \left(\frac{\sigma_x^2}{\sigma_{n_g}^2} \right)^{-1} + \left(\frac{\sigma_x^2}{\sigma_{n_q}^2} \right)^{-1} \quad (24.a)$$

or,

$$\left(\frac{\sigma_x^2}{\sigma_{n_t}^2} \right) = \frac{\left(\frac{\sigma_x^2}{\sigma_{n_g}^2} \right) \cdot \left(\frac{\sigma_x^2}{\sigma_{n_q}^2} \right)}{\left(\frac{\sigma_x^2}{\sigma_{n_g}^2} \right) + \left(\frac{\sigma_x^2}{\sigma_{n_q}^2} \right)}. \quad (24.b)$$

A consequence of this relationship is that the overall SNR is always limited by the partial SNRs, as

$$\left(\frac{\sigma_x^2}{\sigma_{n_t}^2} \right) \leq \min \left\{ \left(\frac{\sigma_x^2}{\sigma_{n_g}^2} \right), \left(\frac{\sigma_x^2}{\sigma_{n_q}^2} \right) \right\} \quad (25)$$

which is easy to deduce from (24.b).

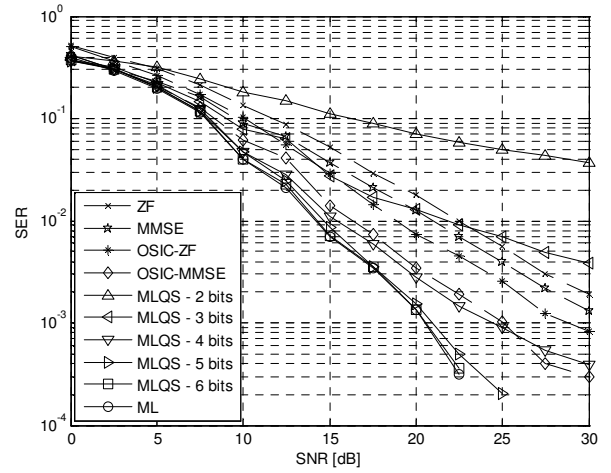


Fig. 5. SER versus average SNR for standard receivers and detection in a quantized space for different levels of quantization per dimension in a 2×2 system using QPSK modulation.

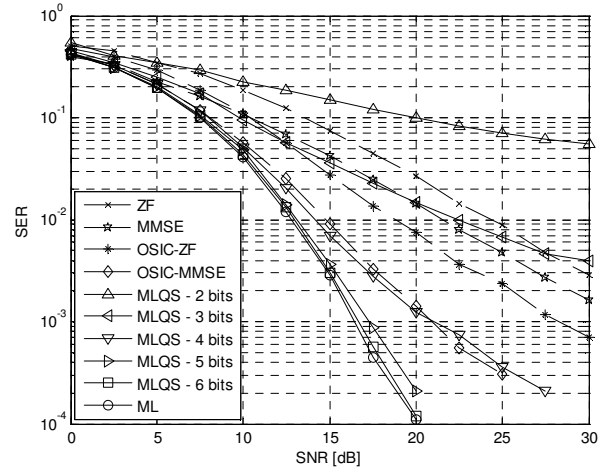


Fig. 6. SER versus average SNR for standard receivers and detection in a quantized space for different levels of quantization per dimension in a 3×3 system using QPSK modulation.

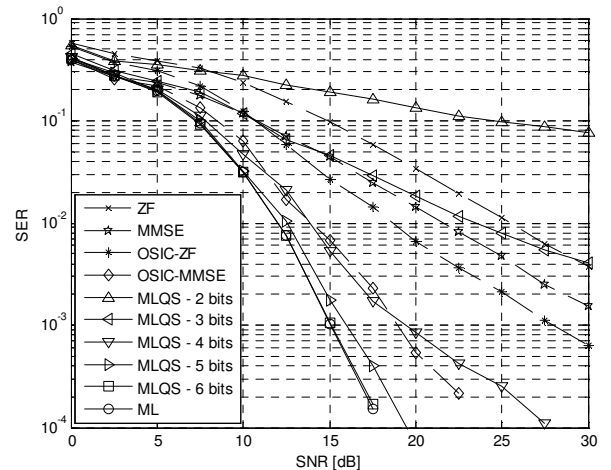


Fig. 7. SER versus average SNR for standard receivers and detection in a quantized space for different levels of quantization per dimension in a 4×4 system using QPSK modulation.

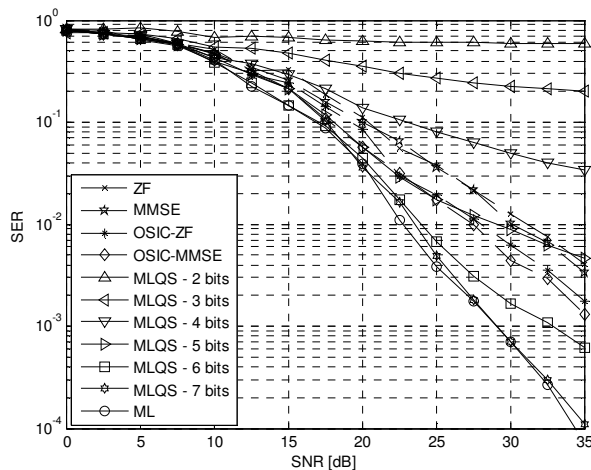


Fig. 8. SER versus average SNR for standard receivers and detection in a quantized space for different levels of quantization per dimension in a 2×2 system using 16-QAM. (A symbol error probability can be >0.5 .)

It is expected that for all transmission schemes as the number of quantization levels increases the SER will meet its lower bound imposed by the Gaussian noise. Conversely, when the quantization noise is dominant, the performance is impaired by an overall SNR that is actually worse than that implied by the horizontal axis of the figures.

The results with QPSK show a similar pattern: for $b=2$ the SER is worse than that for any other receiver; for $b=3$ it is close to the performance of ZF; for $b=4$ it is similar to the performance of OSIC-MMSE; for $b=5$ it is always within 1dB of ML; and for $b=6$ it always coincides with ML. These results show that the total number of bits needed to accurately represent the N_R -dimensional received vector is $5 \times (2 \times N_R)$, i.e., for the most demanding case considered (4×4), 40 bits are needed to obtain near ML performance.

However, it should be observed that for an identical number of lattice points in each dimension ($4^4=16^2=256$) the use of 16-QAM requires a greater number of quantisation bits than does QPSK.

VII. CONCLUSIONS

In each of the $2N_R$ real dimensions of the MIMO spatial detection problem one has M^{N_r} possible points. Hence, the number of multiplications (squares) involved in the ML detection of one received vector is $(2N_R)M^{N_r}$. This paper presents a technique which enables a multiplication-free computation of the components of the squared Euclidean distances by means of a look-up table, which is particularly suitable for VLSI (very large scale integration) architectures. The needed number of bits to represent both the received vectors and the lattice associated with each channel realization is small and could be reduced by quantizing with independently saturations in each real received dimension. Additionally, the number of required pre-stored components constitutes a very small table with only L positions.

The simplified analysis that is presented closely represents the impact of the quantization observed in the simulations: doubling the number of antennas from 2 to 4 originates a

power loss that can be more than compensated by increasing the number of bits per dimension from 5 to 6. Indeed, inspecting the cases in Fig. 5 and Fig. 6 and measuring the energy differences for $\text{BER} < 10^{-3}$, the correct number of additional bits required to maintain performance can be seen to be the predicted “half bit”. In practical systems the number of receive antennas is not expected to be easily doubled from say 4 to 8. Therefore the need for a 6th quantization with QPSK is not required. It should be noticed that the number of comparisons needed remains exponential with the number of transmit antennas, however the overall complexity is reduced.

ACKNOWLEDGMENT

Francisco Monteiro is funded by the Portuguese Foundation for Science and Technology.

REFERENCES

- [1] D. Gesbert, “Breaking the barriers of Shannon’s capacity: An overview of MIMO wireless systems”, *Telenor’s Journal: Elektronik*, Vol. 98, pp. 53–64, Jan. 2002.
- [2] A. J. Paulraj, D. A. Gore, R. U. Nabar and H. Bölcskei, “An overview of MIMO communications - a key to gigabit wireless”, *Proc. of the IEEE*, vol. 92, No. 2, pp. 198–218, Feb. 2004.
- [3] R. W. Heath, Jr., and A. J. Paulraj, “Switching between diversity and multiplexing in MIMO systems”, *IEEE Trans. on Comm.*, Vol. 53, No. 6, pp. 962–968, June 2005.
- [4] T. Kailath, H. Vikalo, B. Hassibi, H. Bölcskei (Editor), D. Gesbert (Editor), C. B. Papadias (Editor), A.-J. van der Veen (Editor), “MIMO receive algorithms”, in *Space-Time Wireless Systems: From Array Processing to MIMO Communications*, Chapter 15, Cambridge University Press, 2006.
- [5] C. Windpassinger, “Detection and precoding for multiple input multiple output channels”, Ph.D. thesis, University of Erlangen-Nuremberg, Nuremberg, Germany, 2004.
- [6] H. Yao and G. W. Wornell, “Lattice-reduction-aided detectors for MIMO communication systems”, in *Proc. of IEEE GLOBECOM’02 – 2002 IEEE Global Telecom. Conf.*, Vol. 1, Taipei, Taiwan, pp. 424–428, Nov. 2002.
- [7] H. Sung, J. W. Kang, K. B. Lee, “A simple maximum likelihood detection for MIMO systems”, *IEICE Trans. on Comm.*, Vol. E89-B, No. 8, pp. 2241–2244, August 2006.
- [8] D. J. Love, R. W. Heath Jr., Wiroonsak Santipach and Michael L. Honig, “What is the value of limited feedback for MIMO channels?”, *IEEE Comm. Magazine*, Vol. 42; No. 10, pp. 54–59, October 2004.
- [9] N. Benvenuto, U. Cherubini, *Algorithms for Communications Systems and their Applications*, Wiley, 2002.
- [10] Y. Ohashi, “Fast linear approximations of Euclidean distances in higher order dimensions”, *Graphics Gems IV*, Morgan Kaufmann, pp. 120–124, 1994.
- [11] M. Barni, F. Buti, F. Bartolini and V. Cappelini “A quasi-Euclidean norm to speed up vector median filtering”, *IEEE Transactions on Image Processing*, Vol. 9, No. 10, pp. 1704–1709, Oct. 2000.
- [12] G. Ferrari, G. Colavolpe, R. Raheli, *Detection Algorithms for Wireless Communications: with Applications to Wired and Storage Systems*, John Wiley and Sons, 2004.
- [13] M. Rupp, G. Gritsch, H. Weinrichter, “Approximate ML detection for MIMO systems with very low complexity”, in *Proc. of ICASP’ 04 – The 2004 IEEE Inter. Conf. on Acoustics, Speech, and Signal Processing*, Vol. IV, pp.809–812, Montreal, Quebec, Canada, 2004.
- [14] S. A. Rizvi, N. M. Nasrabadi, “An efficient Euclidean distance computation for vector quantization using a truncated look-up table”, *IEEE Transactions on circuits and systems for video technology*, Vol. 5, No. 4, pp. 370–371, August 1995.
- [15] C.-C. Chang, J.-S. Chou, T.-S. Chen. “An efficient computation of Euclidean distances using approximated look-up table”, *IEEE Trans. on circuits and systems for video technology*, Vol. 10, No. 4, June 2000.
- [16] M. Magarini and A. Spalvieri, “Performance Evaluation of the V-BLAST Coset Detector”, in *Proc. of ISWCS’05 – 2nd Inter. Symp. on Wireless Comm. Systems*, Sept. 2005, pp. 18-21.